

Zerumbone induces mitochondria-mediated apoptosis via increased calcium, generation of reactive oxygen species and upregulation of soluble histone H2AX in K562 chronic myelogenous leukemia cells

Iyyappan Rajan¹ · P. R. Jayasree¹ · P. R. Manish Kumar¹

Received: 25 March 2015 / Accepted: 18 May 2015 / Published online: 31 May 2015
© International Society of Oncology and BioMarkers (ISOBM) 2015

Abstract Zerumbone, a natural cyclic sesquiterpene, is known to exhibit selective toxicity toward various cancer cells. Sustained efforts to explore the potential of new agents for effective therapy are critical in the context of development of drug resistance especially in cancers like chronic myelogenous leukemia (CML). The present study evaluated the effect of zerumbone on CML-K562 cells. The cell viability of zerumbone-treated K562 cells was detected by MTT assay, and morphological changes were observed by light microscopy and scanning electron microscopy (SEM). Staining with Hoechst 33258, acridine orange/ethidium bromide, and AnnexinV-FITC were used to detect apoptosis. Intracellular reactive oxygen species (ROS), Ca^{2+} , and changes in mitochondrial membrane potential were measured using Dichloro-dihydro-fluorescein diacetate (DCFH-DA), Fluo-3AM, and Rhodamine-123, respectively. Western blot analysis was carried out to detect key proteins involved in apoptosis. Zerumbone inhibited K562 cell proliferation with an IC_{50} value of 3.5 μ g/mL and colony formation capability ($P < 0.001$). Interestingly, zerumbone did not affect the growth of normal human peripheral blood lymphocytes (hPBLs). Distinct morphological changes observed by light microscopy and fluorescent staining with Hoechst-33258, AO/EtBr, annexin V-FITC, and cytotoxicity evaluation by comet

assay indicated induction of DNA damage and apoptosis. This was further confirmed by demonstration of pro-caspase-3, -9 activation and Poly(ADP-ribose) polymerase (PARP) cleavage on western blots. Apoptosis induction was found to be mitochondria mediated, involving increased free intracellular Ca^{2+} , ROS, and upregulation of soluble histone H2AX. Our results suggest that zerumbone holds promise as a potential candidate drug for CML.

Keywords Apoptosis · K562 cells · ROS · Soluble H2AX · Zerumbone

Introduction

Human chronic myelogenous leukemia (CML), a myeloproliferative malignancy, stands out from most other cancers due to its association with a defined genetic alteration—a reciprocal translocation of *c-abl* protooncogene from chromosome 9 to the breakpoint cluster region of *bcr* gene on chromosome 22, leading to the formation of the Philadelphia chromosome (Ph^+) [1]. The BCR-ABL fusion protein is constitutively expressed and as a result; the tyrosine kinase encoded by ABL is highly active in CML cells. It also serves as a model for gene-based, rational design of anticancer therapy. However, the use of the first-generation tyrosine kinase inhibitor (TKI), imatinib mesylate, though initially successful in treating CML, was soon found to be marred by the development of resistance in the patients toward the drug mainly due to acquisition of mutations in the BCR-ABL kinase domain. As this

✉ P. R. Manish Kumar
manishramakrishnan@rediffmail.com

¹ Department of Biotechnology, University of Calicut, Malappuram, Kerala 673 635, India

was a consequence of long-term monotherapy, cessation or change of therapy has been recently reported [2]. Resistance continues to be encountered even with the use of second-generation TKIs such as dasatinib, nilotinib, and ponatinib which target specific mutations associated with drug resistance. In this scenario, sustained efforts are required to explore the potential of new agents applied singly or in combination for effective anticancer therapy.

Plants have been exploited as a bioresource for many therapeutic drugs for treating various ailments including cancer [3, 4]. The therapeutic benefits emanate from the structural diversity of phytochemicals contained therein which possess diverse, pharmacologically active compounds [5]. Plant-based compounds continue to play a major role in anticancer drug development. Zerumbone, a natural cyclic sesquiterpene from *zingiber zerumbet*, reported to have a diverse range of biological activities [6], including anticancer and antitumor activities [7, 8], has attracted researchers as it also exhibits selective toxicity toward cancer cells compared to normal cells [9]. Zerumbone-induced apoptosis involving different signaling pathways have been reported in various cell lines [6]. In the present study, we have evaluated the antiproliferative and apoptosis-inducing effect of zerumbone on K562 cells.

Materials and methods

Chemical reagents

Zerumbone, (5-bromo-4-chloro-3'-indolylphosphate/nitroblue tetrazolium) BCIP/NBT, Dimethyl sulfoxide (DMSO), Dichloro-dihydro-fluorescein diacetate (DCFH-DA), rhodamine-123, Fluo-3AM, methylcellulose, annexin V-FITC apoptosis detection kit, propidium iodide, anti-H2A-X, anti- γ H2A-X, and anti-actin antibodies were purchased from Sigma-Aldrich (St. Louis, MO, USA). Anti-caspase-3, -9 and anti-PARP were purchased from Cell Signaling Technology, USA. Tris base, (4-(2-hydroxyethyl)-1-piperazineethanesulfonic acid) HEPES, glycine, acridine orange, ethidium bromide, and triton X-100 were purchased from SRL Pvt. Ltd., Mumbai, India. Goat anti-rabbit IgG-ALP conjugate, Goat anti-mouse IgG-ALP conjugate, and agarose were procured from Genei, Bangalore, India. Fetal bovine serum (FBS), RPMI-1640, HiSep™ LSM lymphocyte separation medium, and HiKaryoXL™ RPMI medium were purchased from HiMedia Laboratories Pvt. Ltd, Mumbai, India. Positively charged nylon membrane was purchased from BDH laboratory supplies, England. All other chemicals and reagents used were of analytical grade.

Cells and culture conditions

The human K562 cell line was cultured in RPMI-1640 medium supplemented with FBS (10 %, v/v), HEPES (25 mM), streptomycin (100 μ g/mL), and penicillin (100 U/mL) in CO₂ humidified atmosphere at 37 °C. Human peripheral blood lymphocytes (hPBLs) were cultured using HiKaryoXL™ RPMI medium according to the manufacturer's protocol. Giemsa-stained chromosome spreads prepared from lymphocytes were used for the determination of mitotic index (MI) calculated as the percentage of cells undergoing mitosis [10]. MI is a standard means to determine the proliferation status of cell populations such as hPBLs in response to compounds that inhibit or induce cell division. The number of metaphases per thousand cells was scored to determine the MI.

Cell viability assay

K562 cells (2×10^4 cells/well) were seeded into 96-well plates and cultured overnight. For lymphocytes, 48-h cultures were used for treatment. The cells were treated with different concentrations of zerumbone. Cells treated with equivalent amounts of the solvent DMSO were used as negative control. After incubation for 24, 48, and 72 h, MTT assay was performed as described by Mosmann [11].

Clonogenic assay

K562 cells were treated with zerumbone for 24 h at 37 °C in a humidified incubator and subsequently used for clonogenic assay [12]. Briefly, the control and treated cells (1×10^3) were washed with PBS (pH 7.4), mixed with semi-solid methylcellulose culture medium [complete RPMI-1640 medium containing 0.8 % (w/v) methylcellulose], and then plated into a 6-well dish. After a 10-day incubation period, the colonies were stained with crystal violet (0.5 % w/v) and then counted using an inverted microscope.

Comet assay

The comet assay was performed under alkaline conditions. The control and zerumbone-treated cells were subjected to alkaline gel electrophoresis as per Singh et al. [13]. The slides were stained with ethidium bromide (10 μ g/mL) for 10 min and observed under fluorescence microscope.

Light microscopy

K562 cells (1×10^6) were treated with different concentrations of zerumbone for 24 h. The control and treated cells were harvested and washed with ice-cold PBS and

then visualized through phase-contrast inverted microscope to note the morphological differences.

Scanning electron microscopy (SEM)

The control and treated cells were fixed with 2.5 % (*v/v*) glutaraldehyde at room temperature for 1 h, washed in 1× PBS, and exposed to 1 % (*w/v*) osmium tetroxide for another hour. They were then dehydrated by sequential immersion in an ascending (10 % increment) graded series of alcohol ranging from 10 to 90 %, followed by two changes in absolute alcohol. The dried cells were then coated with gold and observed with a Hitachi SU 6600 scanning electron microscope [14].

Hoechst 33258 staining

Cells (1×10^6) were seeded into 24-well plates and treated with various concentrations of zerumbone for 24 h. After collection, the cells were washed twice with PBS and re-suspended in the Hoechst 33258 solution (1 mg/mL). The cells were then observed through a fluorescence microscope and imaged using cool CCD camera.

Acridine orange/ethidium bromide staining

Apoptosis and cell viability were determined by differential staining with ethidium bromide/acridine orange [15]. The control and treated cells were harvested and centrifuged at $800 \times g$. The cell pellets were washed with cold PBS and adjusted to a cell density of 2×10^5 cells/mL using PBS. The acridine orange/ethidium bromide (AO/EtBr) solution (1:1, *v/v*) was added to the cell suspension at a final concentration of 100 $\mu\text{g/mL}$. The cells were then observed under a fluorescence microscope.

Study of phosphatidylserine externalization

Phosphatidylserine (PS) externalization in control and treated cells (1×10^6) was analyzed using annexin V-FITC apoptosis detection kit according to the manufacturer's instruction. The cells were mounted on slides, and the images were captured to observe the cells undergoing apoptosis.

Assessment of intracellular reactive oxygen species

Intracellular ROS was measured using the dye, Dichloro-dihydro-fluorescein diacetate (DCFH-DA)-based assay [16, 17]. Both the control and treated cells were incubated with 10 μM DCFH-DA at 37 °C for 30 min and then washed twice with PBS followed by observation under fluorescence microscope, and ROS

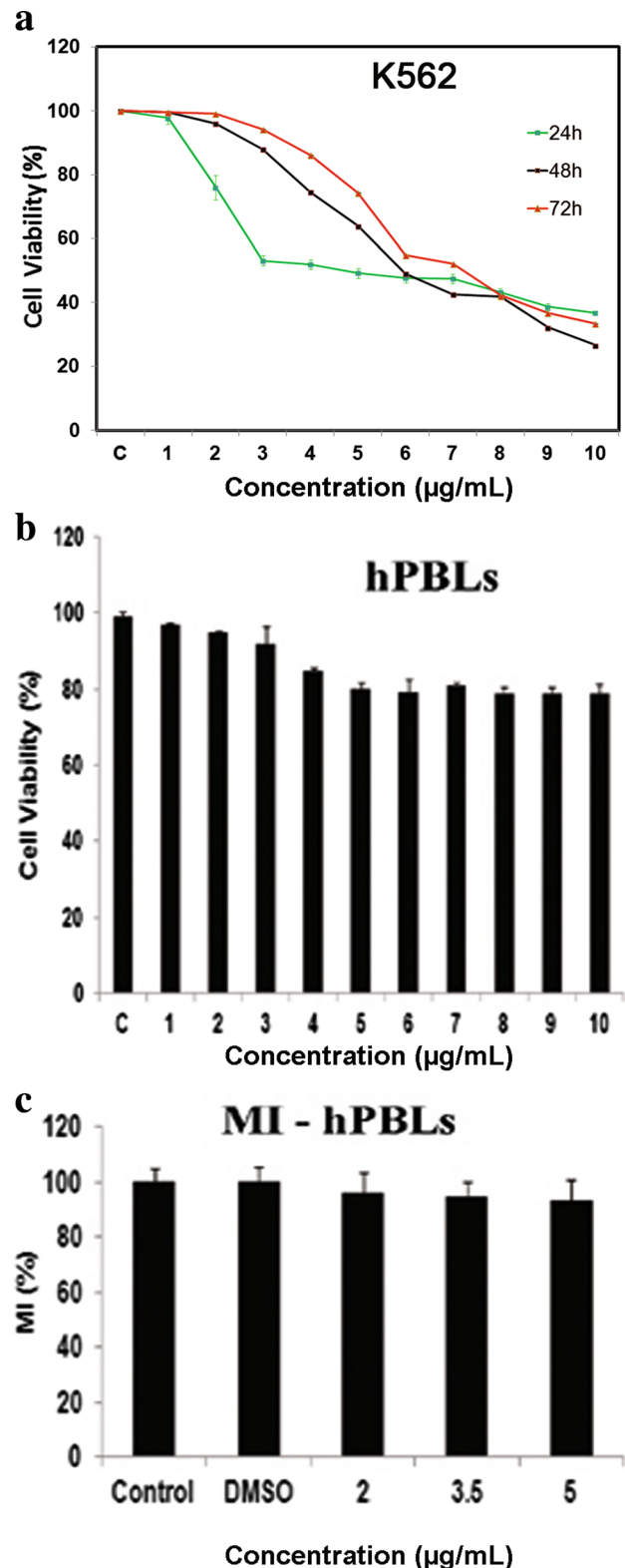


Fig. 1 Effect of zerumbone on K562 cells and normal hPBLs. **a** Cell viability of K562 cells was assessed by the MTT method after 24-, 48-, and 72-h treatment. **b** Cell viability of normal hPBLs was assessed by the MTT method after 24-h treatment. Viable cell count was determined taking untreated controls as 100 %. **c** Mitotic index of cultured hPBLs. Data shown as mean \pm SD of three independent experiments

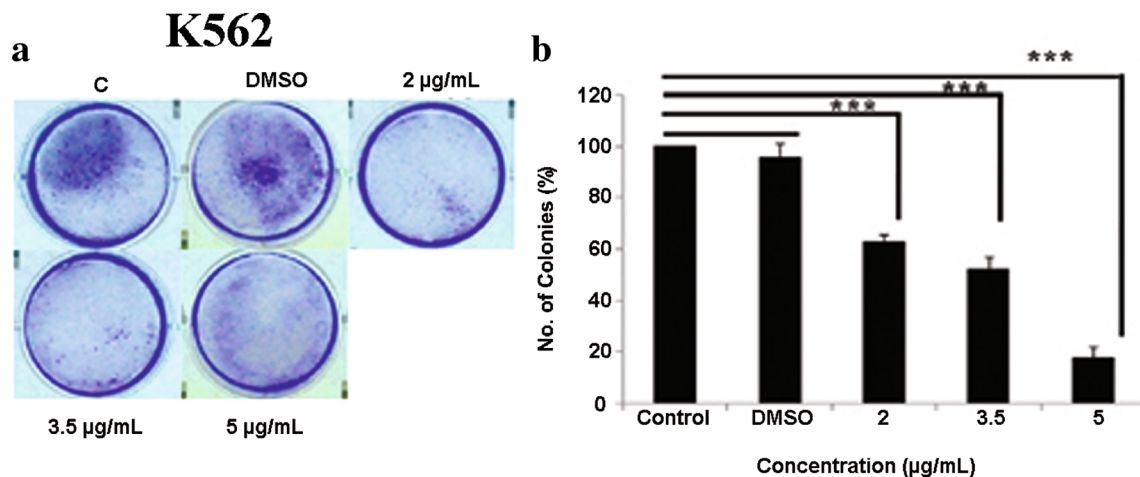


Fig. 2 **a** Clonogenic capacity in zerumbone-treated K562 cells as measured by colony-forming assay stained with crystal violet. **b** The number of colonies in zerumbone-treated K562 cells was significantly

reduced compared with that of untreated control. Data shown as mean \pm SD of three independent experiments. *** P <0.001 compared with the untreated control group

was measured using a flow cytometer and analyzed with BD FACS Diva software version 5.0.2.

mitochondria observed under fluorescence microscope was measured by flow cytometry with BD FACS Diva software version 5.0.2 [18].

Measurement of mitochondrial membrane potential

K562 cells were seeded (1×10^6) into six-well plates and cultured with or without zerumbone (2 to 5 $\mu\text{g/mL}$) for 24 h. After treatment, cells were incubated with the lipophilic cationic dye Rhodamine 123 (10 $\mu\text{g/mL}$) for 30 min. Cells were then harvested and washed with PBS. The green fluorescence from the depolarized

Analysis of intracellular Ca^{2+} concentration

Changes in intracellular Ca^{2+} concentrations were determined by a fluorescent dye, Fluo-3AM. Cells were washed twice with PBS and incubated with 5 μM Fluo-3AM at 37 $^\circ\text{C}$ for 30 min. The cells were then washed and subjected to FACS analysis [19].

Fig. 3 Morphological changes in K562 cells after 24-h treatment with zerumbone at different concentrations. Representative images taken using **a** light microscopy and **b** SEM. Fluorescence microscopy images of K562 cells stained with **c** Hoechst 33258; *arrow heads* indicate apoptotic nuclear condensation and DNA fragmentation. *Scale bars*: 15 μm for all images

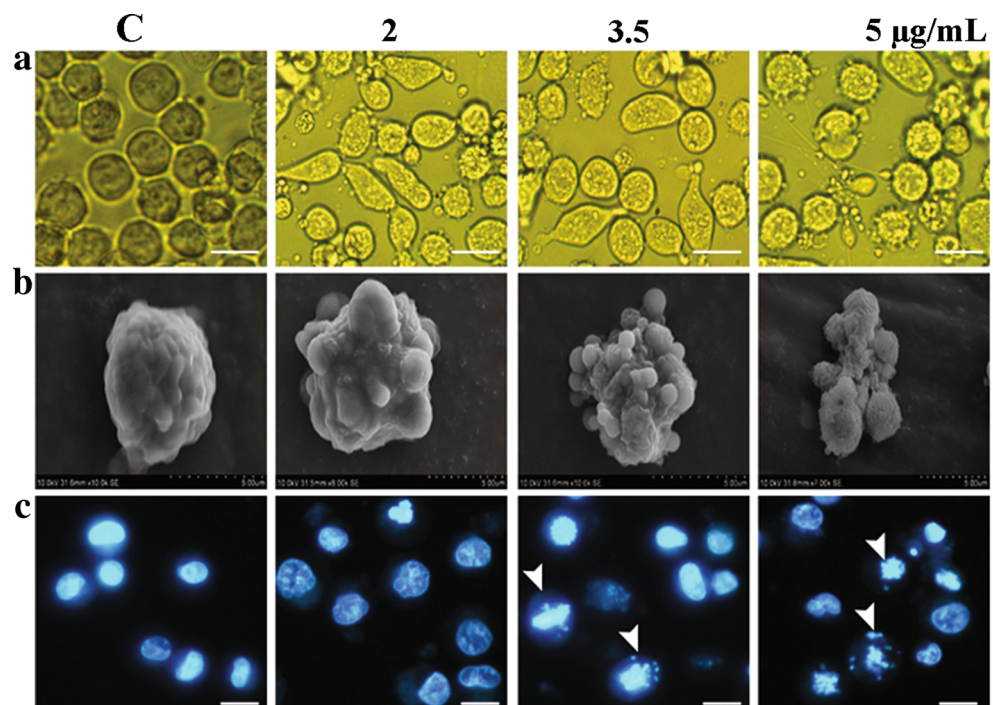
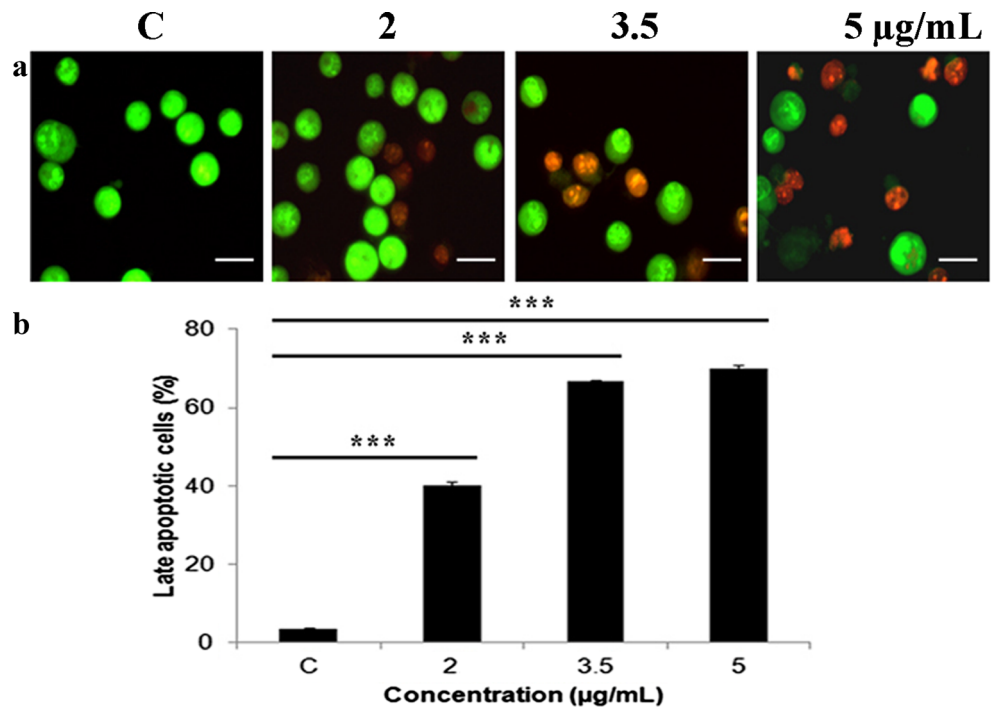


Fig. 4 Effect of zerumbone on K562 cells after 24-h treatment. Fluorescence microscopy images of K562 cells stained with **a** AO/EtBr and its **b** quantitative analysis of late apoptotic cells. *Scale bars*: 15 μ m for all images. Data shown as mean \pm SD of three independent experiments. * P <0.05, ** P <0.0, *** P <0.001 compared with the untreated control group



Western blot analysis

The control and zerumbone-treated cells were washed with cold PBS and lysed in RIPA buffer containing protease/phosphatase inhibitors. The protein concentration was measured using Bradford method. Proteins (50 μ g) were fractionated on a 12.5 % SDS-PAGE gel

and then transferred onto a positively charged nylon membrane. Membranes were blocked (1 h, room temperature) in 3 % BSA in TBS, incubated (overnight, 4 $^{\circ}$ C) with the following primary antibodies separately (dilution 1:1000): anti-Caspase-3, anti-Caspase-9, anti-PARP, anti-actin, anti- γ H2A-X, and anti-H2A-X. The membranes were then washed in TBS and incubated

Fig. 5 Effect of zerumbone on K562 cells after 24-h treatment. Fluorescence microscopy images of K562 cells stained with **a** Annexin V-FITC/PI and its **b** quantitative analysis of late apoptotic cells. *Scale bars*: 15 μ m for all images. Data shown as mean \pm SD of three independent experiments. * P <0.05, ** P <0.0, *** P <0.001 compared with the untreated control group

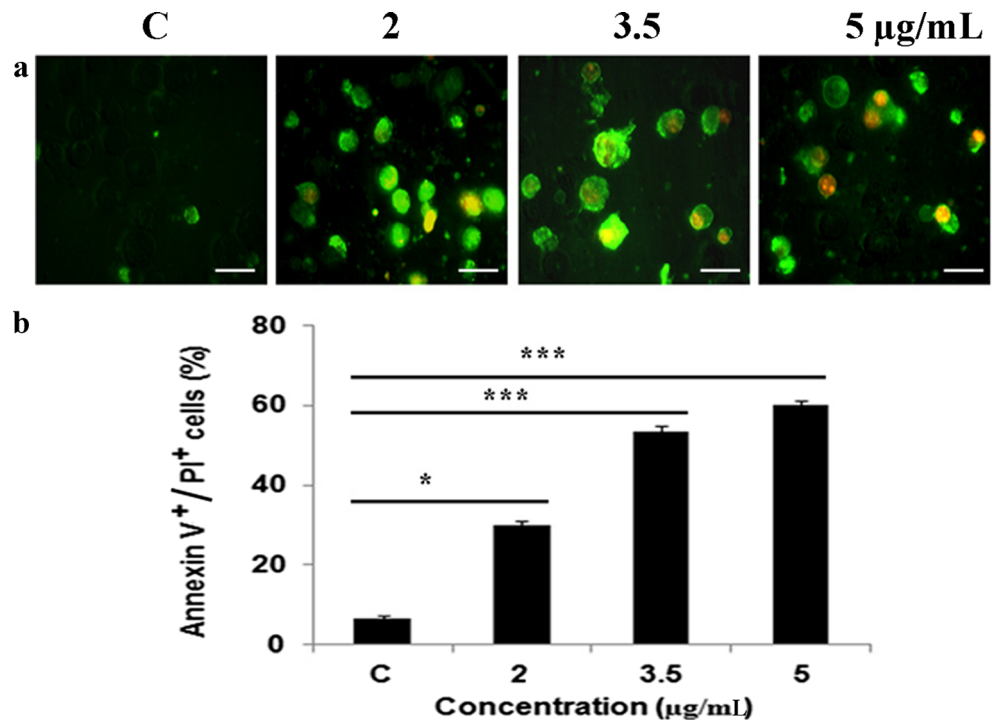
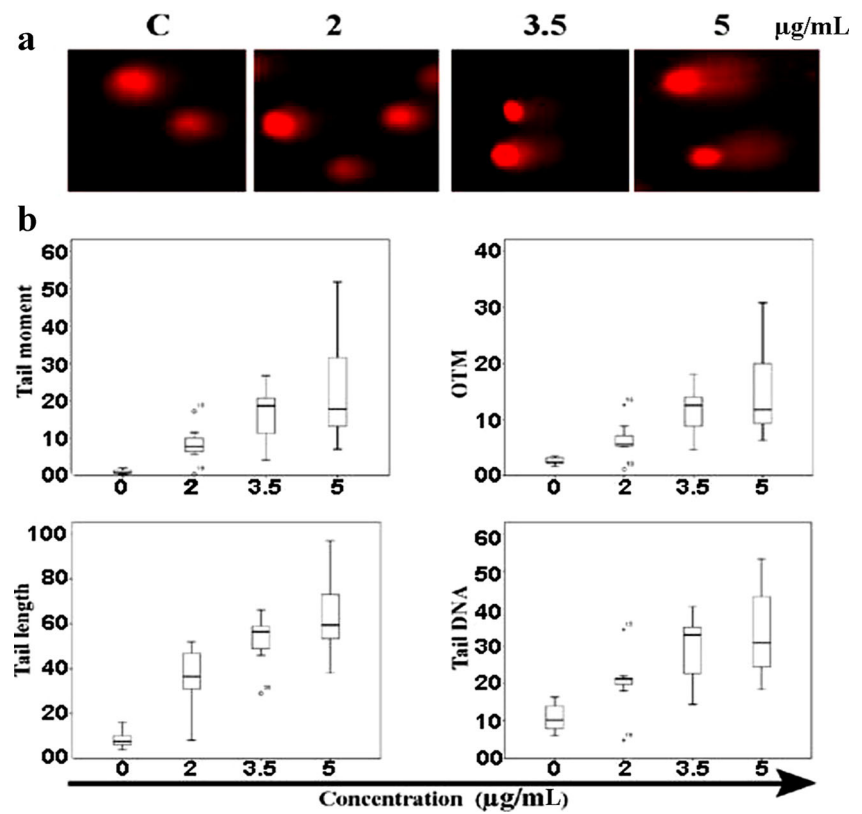


Fig. 6 Detection of DNA damage by alkaline comet assay in K562 cells after treatment with zerumbone at different concentrations for 24 h. **a** Images of comets taken after treatment with zerumbone. **b** Quantitative analysis of the comets using CASP software. *Box-and-Whisker* plots represent results for ten comets, each taken from a different concentration. The percentage of DNA in the tail moment (TM), olive tail moment (OTM), tail length (TL), and comet tail DNA (TDNA%) was recorded to characterize DNA damage



(1 h, room temperature) with ALP-conjugated secondary antibody which was either anti-mouse or anti-rabbit (1:2000). Membranes were then washed and visualized with BCIP/NBT solution [20].

Statistical analysis

The data are expressed as the mean±SD from three independent experiments. Results were analyzed for

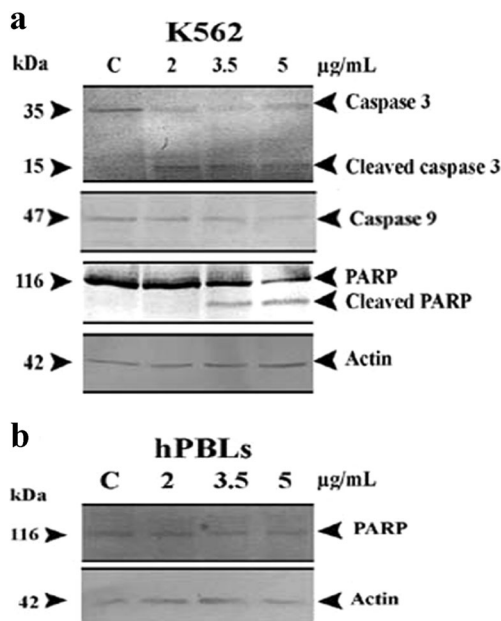


Fig. 7 **a** Proteolytic cleavage of PARP and activation of caspase-3, -9 was analyzed in zerumbone-treated K562 cells by immunoblotting. **b** No PARP cleavage was observed in hPBLs. β -actin was used as a loading control

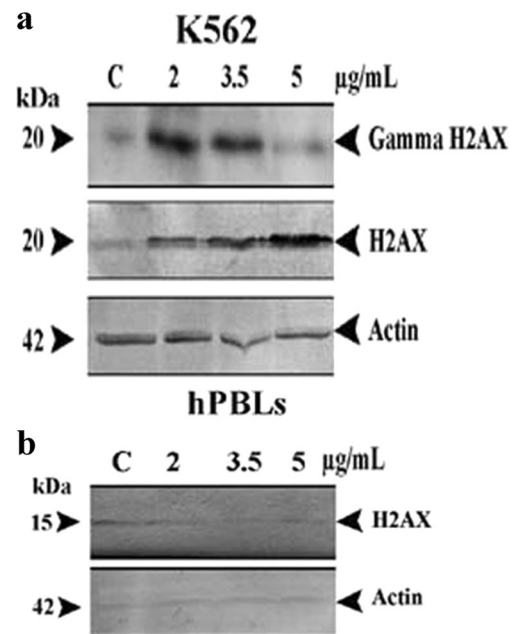


Fig. 8 **a** Upregulation of γ H2AX and soluble H2AX protein levels were observed in zerumbone-treated K562 cells. **b** Soluble H2AX was not affected in hPBLs after treatment with zerumbone. β -actin was used as a loading control

significance by one-way ANOVA using SPSS software version 16.0. Differences with $P < 0.05$ were considered significant. Asterisks (*) were used to identify the level of significance ($*P \leq 0.05$, $**P \leq 0.01$, and $***P \leq 0.001$).

Results

Zerumbone inhibits proliferation of K562 cells but not that of hPBLs

The effect of zerumbone on the proliferation of K562 cells and hPBLs was measured by the MTT assay. Treatment of K562 cells with zerumbone for 24, 48, and 72 h at different concentrations (1–10 $\mu\text{g}/\text{mL}$) resulted in significant inhibition of cell growth in comparison to untreated (control) cells. After 24-h treatment, up to 50 % of growth reduction was observed to be dose-dependent within the concentration range of 1–3 $\mu\text{g}/\text{mL}$, IC_{50} value being 3.5 $\mu\text{g}/\text{mL}$. Beyond this, up to 10 $\mu\text{g}/\text{mL}$, further growth reduction was not concentration-dependent and was found to be less than 15 % only. Prolonged treatment with zerumbone (48 and 72 h), however, did not result in

increased cell death (Fig. 1a). Hence, further analysis was carried out only on 24-h treated cells. On the other hand, growth reduction in hPBLs was affected minimally by zerumbone after 24-h treatment at the concentrations tested (Fig. 1b). In DMSO-treated K562 cells and hPBLs, only less than 10 % reduction in growth was observed at the maximum concentration tested (data not shown). The mitotic indices showed that zerumbone treatment did not inhibit proliferation of normal hPBLs (Fig. 1c). Likewise, clonogenic or colony-forming potential of cells is routinely evaluated to determine cell's reproductive ability. Our results showed that zerumbone-treated K562 cells displayed a concentration-dependent reduction in colony formation capability compared to that of untreated control cells, indicating that zerumbone effectively suppressed growth and proliferation of these cells (Fig. 2a, b).

Zerumbone changes cell morphology and induces cell death in K562 cancer cells

Observations of cells by light microscopy and the scanning electron microscopy demonstrated that zerumbone-treated

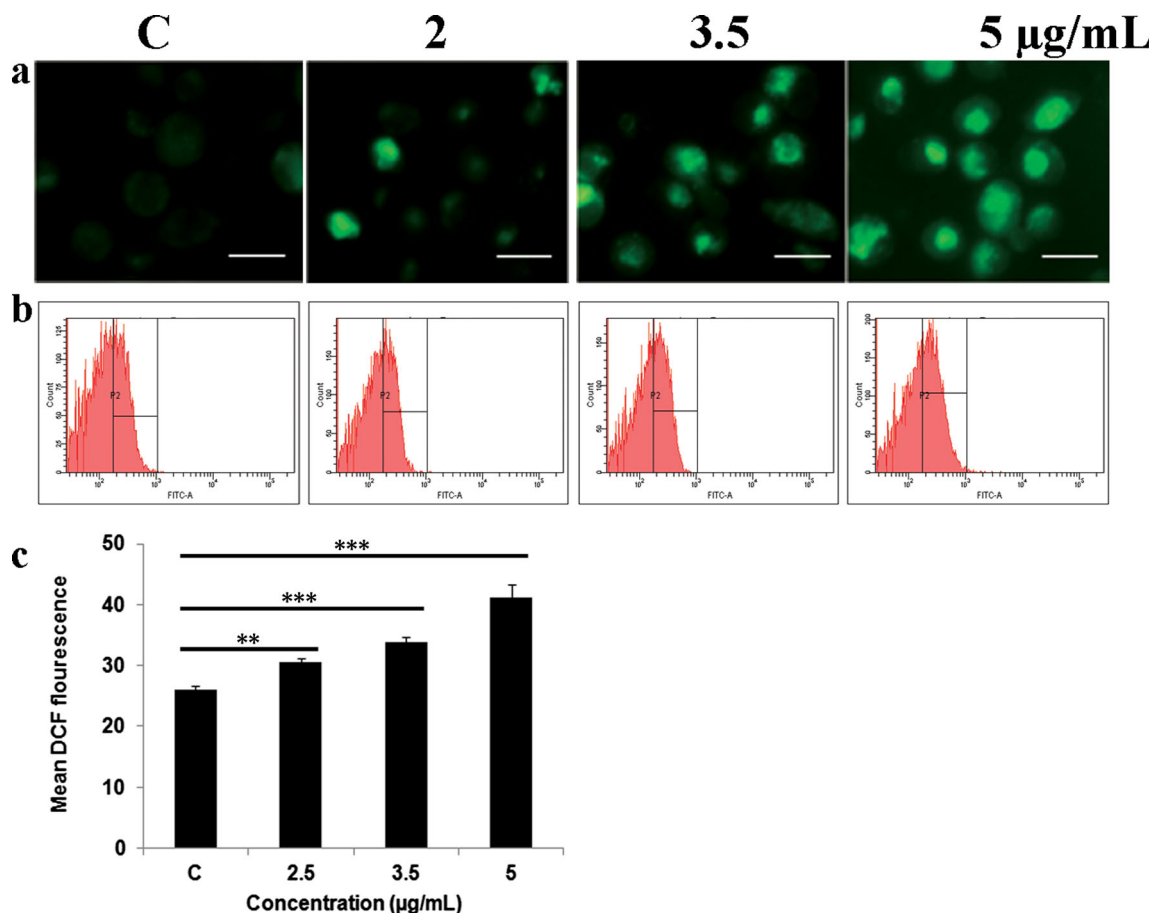


Fig. 9 Effect of zerumbone on K562 cells after 24-h treatment. **a** Microscopic images, **b** flow cytometric analysis, and **c** mean fluorescence intensity of K562 cells stained with ROS indicator DCFH-

DA. Scale bars: 15 μm for all images. Data shown as mean \pm SD of three independent experiments. $*P < 0.05$, $**P < 0.01$, $***P < 0.001$ compared with the untreated control group

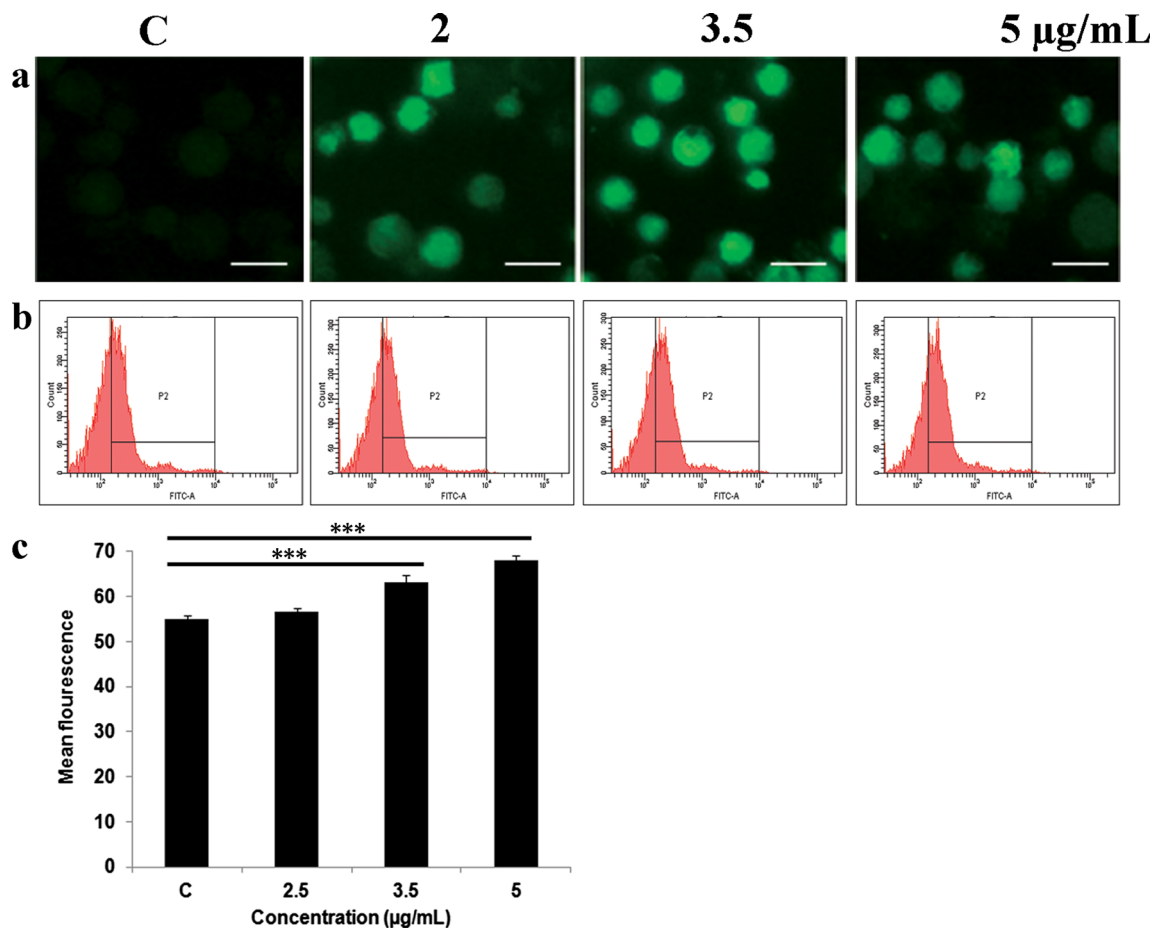


Fig. 10 Effect of zerumbone on K562 cells after 24-h treatment. **a** Microscopic images, **b** flow cytometric analysis, and mean **c** fluorescence intensity of K562 cells stained with Ca indicator Fluo-

3AM. Scale bars: 15 µm for all images. Data shown as mean±SD of three independent experiments. * $P<0.05$, ** $P<0.01$, *** $P<0.001$ compared with the untreated control group

cells displayed distinct morphological changes. While many cells were observed to assume a more or less “sausage” or “spindle” shape at concentrations below 3.5 µg/mL, changes such as cell shrinkage, extensive membrane blebbing, and cellular fragmentation were more evident at higher concentrations tested up to 5 µg/mL (Fig. 3a, b). Induction of such spindle-shaped cells has been observed in K562 cells treated with a synthetic compound, MZ3, apparently due to its interference with microtubule assembly [21]. Chromatin condensation and nuclear fragmentation were also seen on staining cells with the nuclear stain, Hoechst 33258 (Fig. 3c). Further, to determine whether these morphological changes were associated with induction of cell death, AO/EtBr and annexin V-FITC/PI staining was carried out. The characteristic green fluorescence emitted by untreated cells, yellow by early apoptotic, and orange by late apoptotic cells were observed in zerumbone-treated cells (Fig. 4a, b, $P<0.001$). Zerumbone-induced, concentration-dependent increase in the number of annexin V positive cells was

also observed which enabled better determination of apoptosis in K562 cells (Fig. 5a, b, $P<0.001$).

Zerumbone induces DNA damage, caspase-3, -9 activation, and PARP cleavage in K562 cells

The comet assay is a rapid, simple, and sensitive method for measuring DNA damage at the single cell level [22]. Based on the four parameters considered for the assessment of DNA damage, namely, tail moment, olive tail moment, tail length, and tail DNA%, our data showed a proportionate increase in all of the four attributes indicating that zerumbone induces DNA damage in a concentration-dependent manner (Fig. 6a, b, $P<0.001$). To confirm induction of apoptosis by zerumbone, we analyzed the canonical hallmarks, namely, proteolysis of PARP protein and caspase-3, -9 activation in K562 cells by western blot. We found evidence of the expression of 116-kDa PARP and its partial cleavage to the characteristic 85-kDa fragment in addition to activation of pro-

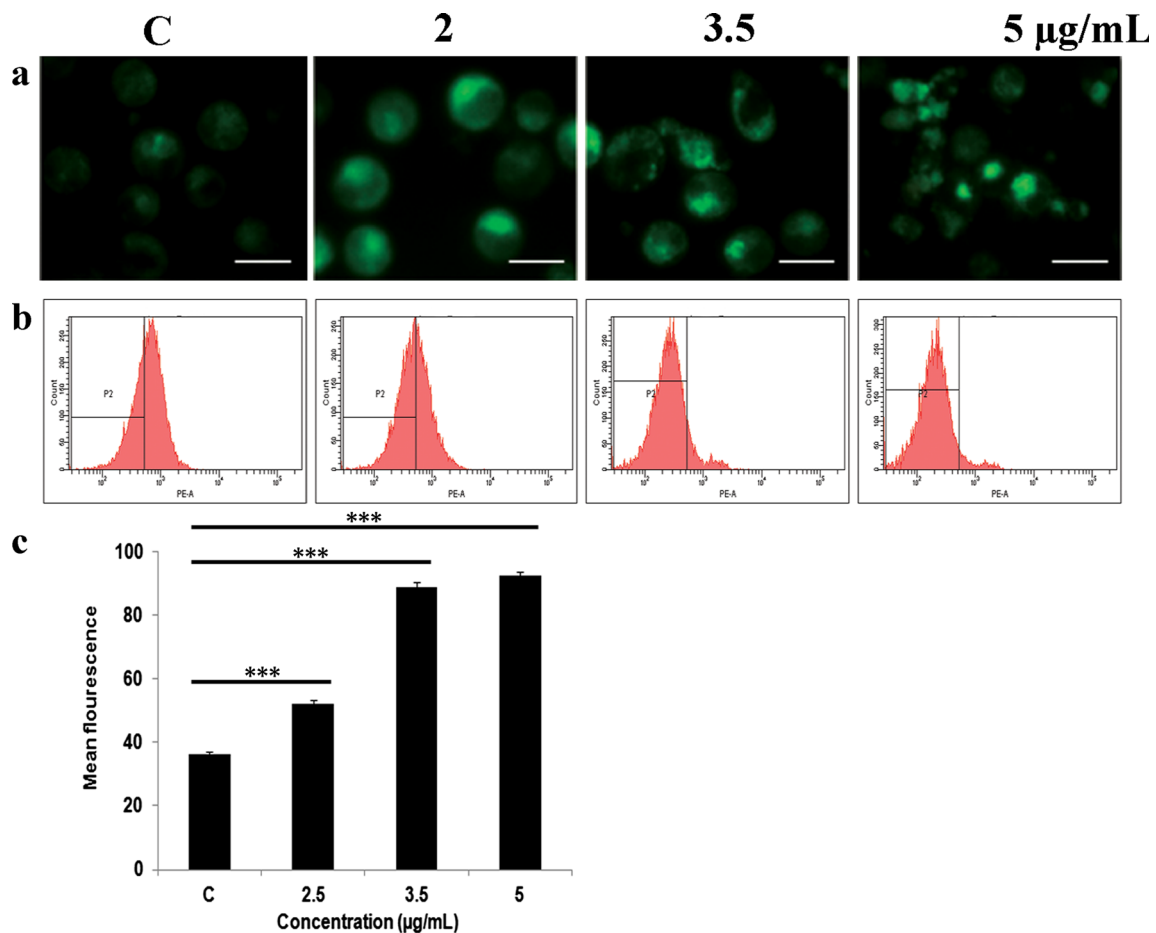


Fig. 11 Effect of zerumbone on K562 cells after 24-h treatment. **a** Microscopic images, **b** flow cytometric analysis, and **c** mean fluorescence intensity of K562 cells stained with mitochondrial-specific, voltage-dependent fluorescent probe, Rhodamine-123. Scale

bars: 15 µm for all images. Data shown as mean±SD of three independent experiments. * P <0.05, ** P <0.0, *** P <0.001 compared with the untreated control group

caspase-3 and -9 in zerumbone-treated K562 cells; however, PARP cleavage was not observed in hPBLs (Fig. 7c, d).

Zerumbone induces increase in levels of γ H2AX and upregulates soluble H2AX expression in K562 cells

It is well established that in the event of DNA damage, H2AX assumes critical importance in influencing the cell's decision to repair DNA or induce apoptosis. DNA double-strand breaks are known to induce phosphorylation of the histone variant H2AX to γ H2AX [23]. Western blot analysis showed that the levels of γ H2AX increased in K562 cells treated with lower doses (2 and 3.5 µg/mL) and decreased in those treated with a higher dose (5 µg/mL). Recent studies have highlighted a link between increased non-chromatin soluble H2AX and apoptosis induction [24]. We observed a conspicuous increase in the levels of this protein in zerumbone-treated cells, in a concentration-dependent manner, while no

difference could be found in the levels of the protein in hPBLs (Fig. 8a, b).

Zerumbone increases intracellular Ca^{2+} , ROS production, and mitochondrial membrane potential loss

The parameters such as intracellular calcium, ROS, and change in the mitochondrial membrane potential, widely implicated in apoptosis induction [25–27], were assessed in order to ascertain their involvement in zerumbone-induced apoptosis in K562 cells. Increased fluorescence intensity was observed in response to the levels of free intracellular Ca^{2+} and ROS using calcium indicator Fluo-3AM and DCFH-DA, respectively. Similarly, increased fluorescence of mitochondria-specific and voltage-dependent fluorescent probe, Rhodamine-123, was also observed which indicated loss in mitochondrial membrane potential. In all the three cases, the increase in fluorescence was dose-dependent (Figs. 9, 10, and 11). These results indicated that zerumbone-induced apoptosis

was mediated through calcium, ROS, and loss of mitochondrial membrane potential in K562 cells.

Discussion

The use of natural anticancer agents, in comparison to their synthetic counterparts, has been regarded to be relatively safe pharmaceutically as they are non-toxic or exert minimal cytotoxicity [28]. Zerumbone is one such compound which has recently been hailed to possess tremendous anticancer potential as it exhibits selective toxicity toward cancer cells compared to normal cells [9].

In the present study, we have evaluated the antiproliferative and apoptosis-inducing effect of zerumbone on CML K562 cells and normal hPBLs. The results of MTT and clonogenic assay showed that zerumbone inhibited proliferation and growth of K562 cells. Interestingly, both MTT assay and MI of zerumbone-treated normal hPBLs failed to show discernible deleterious effects. These results are significant as they confirm the selective killing property of zerumbone, at the concentrations tested in this study, with respect to K562 cells. At higher doses (40 and 80 μM), however, zerumbone has been reported to be cytotoxic but not clastogenic in hPBLs [29] while exerting minimal effects at 13 and 50 μM on growth of normal human dermal (2F0-C25) and colon (CCD-18 Co) fibroblasts [9]. We have also provided clear morphological evidences associated with apoptosis such as cell shrinkage, dynamic membrane blebbing, chromatin condensation, and nuclear fragmentation indicating that zerumbone induces apoptosis in K562 cells.

Further, our results showed that zerumbone treatment in K562 cells not only induced DNA double-stranded breaks in a concentration-dependent manner as evidenced by comet assay but also additionally resulted in caspase-3 and -9 activation which is primarily responsible for PARP cleavage. Calcium and reactive oxygen species constitute two important signaling molecules which have been implicated in the induction of apoptosis [27]. Enhanced entry and release of calcium from ER and mitochondria have been shown to result in disruption of intracellular calcium homeostasis [25, 30]. Mitochondrial calcium uptake and overload has also been linked with enhanced ROS generation, opening of permeability transition pore, release of cytochrome *c* followed by caspase-3 activation and apoptosis [25, 27, 31]. Our results showed that zerumbone treatment significantly increased the levels of intracellular calcium, ROS, and loss of mitochondrial membrane potential. An increase in intracellular cytosolic calcium due to calcium release from ER in zerumbone-treated cells has already been reported [32].

The status of histone H2AX phosphorylation is a key determinant which regulates the cell's response in either repairing the damaged DNA for survival or undergoing

apoptosis [23]. As expected, following zerumbone treatment in K562 cells, the levels of γH2AX were found to increase. But this was true only with respect to lower concentrations tested (2 and 3.5 $\mu\text{g/mL}$); at a dose of 5 $\mu\text{g/mL}$ beyond the IC_{50} value, however, the level of γH2AX was found to be decreased for reasons that remain unclear to us. But results of the comet assay show that zerumbone induces concentration-dependent increase in DNA double-strand breaks. However, analysis of total H2AX protein expression by immunoblotting clearly showed its upregulation on zerumbone treatment in a dose-dependent manner. This is in agreement with reports showing apoptosis induction mediated through upregulation of H2AX following Bortizomib and Imatinib mesylate treatment in Gastrointestinal stromal tumor (GIST) cells. It has also been reported that DNA replication stress leads to upregulation of soluble histone H2AX and that chromatin-associated H2AX sensitizes cells to undergo apoptosis [24, 33, 34]. Interestingly, Kang et al. [35] has recently demonstrated that DNA damage induces ROS through overexpression of histone H2AX. Our results also corroborate that increased H2AX is linked with increased ROS production in zerumbone-treated cells.

The present study has revealed that zerumbone treatment in K562 cells induces apoptosis through mitochondrial mediated pathway linked to upregulation of total histone H2AX, increased calcium and ROS production. Considering our results, zerumbone holds promise as a potential candidate drug for CML.

Acknowledgments The authors wish to thank the Director, Rajiv Gandhi Centre for Biotechnology (RGCB), Thiruvananthapuram, for allowing the use of their FACS facility. Thanks are due to Dr. Ruby John Anto (RGCB) for gifting us with K562 cells, Mrs Indu Ramachandran (RGCB) for the technical help with FACS, and the National Institute of Technology, Calicut, for the SEM analysis. Financial assistance to JPR through Govt. of India—Dept of Biotechnology—BioCARE Scheme is gratefully acknowledged. Technical assistance by Ms. Soumya T. is also acknowledged.

Conflicts of interest None.

References

1. Bunz F. Cancer genetics in the clinic. In: Principles of cancer genetics. New York: Springer; 2008.
2. Parker W, Yeoman A, Jamison B, Yeung D, Scott H, Hughes T, et al. BCR-ABL1 kinase domain mutations may persist at very low levels for many years and lead to subsequent TKI resistance. *Br J Cancer*. 2013;109:1593–8.
3. Cragg GM, Newman DJ. Plants as a source of anti-cancer agents. *J Ethnopharmacol*. 2005;100:72–9.
4. Cragg GM, Grothaus PG, Newman DJ. Impact of natural products on developing new anti-cancer agents. *Chem Rev*. 2009;109:3012–43.
5. Dillard CJ, German JB. Phytochemicals: nutraceuticals and human health. *J Sci Food Agric*. 2000;80:1744–56.

6. Prasannan R, Kalesh KA, Shanmugam MK, Nachiyappan A, Ramachandran L, Nguyen AH, et al. Key cell signaling pathways modulated by zerumbone: role in the prevention and treatment of cancer. *Biochem Pharmacol*. 2012;84:1268–76.
7. Huang GC, Chien TY, Chen LG, Wang CC. Antitumor effects of zerumbone from *Zingiber zerumbet* in P-388D1 cells *in vitro* and *in vivo*. *Planta Med*. 2005;71:219–24.
8. Zhang S, Liu Q, Liu Y, Qiao H, Liu Y. Zerumbone, a southeast Asian Ginger Sesquiterpene, induced apoptosis of pancreatic carcinoma cells through p53 signaling pathway. *Evid Based Complement Alternat Med*. 2012;2012:8.
9. Murakami A, Takahashi D, Kinoshita T, Koshimizu K, Kim HW, Yoshihiro A, et al. Zerumbone, a Southeast Asian ginger sesquiterpene, markedly suppresses free radical generation, proinflammatory protein production, and cancer cell proliferation accompanied by apoptosis: the α , β -unsaturated carbonyl group is a prerequisite. *Carcinogenesis*. 2002;23:795–802.
10. Eke D, Celik A. Genotoxicity of thimerosal in cultured human lymphocytes with and without metabolic activation sister chromatid exchange analysis proliferation index and mitotic index. *Toxicol in Vitro*. 2008;22:927–34.
11. Mosmann T. Rapid colorimetric assay for cellular growth and survival: application to proliferation and cytotoxicity assays. *J Immunol Methods*. 1983;65:55–63.
12. Franken NA, Rodermond HM, Stap J, Haveman J, Van Bree C. Clonogenic assay of cells *in vitro*. *Nat Protoc*. 2006;1:2315–9.
13. Singh NP, McCoy MT, Tice RR, Schneider EL. A simple technique for quantitation of low levels of DNA damage in individual cells. *Exp Cell Res*. 1988;175:184–91.
14. Subhashini J, Mahipal SV, Reddy MC, Mallikarjuna Reddy M, Rachamalla A, Reddanna P. Molecular mechanisms in C-Phycocyanin induced apoptosis in human chronic myeloid leukemia cell line-K562. *Biochem Pharmacol*. 2004;68:453–62.
15. Kasibhatla S, Amarante-Mendes GP, Finucane D, Brunner T, Bossy-Wetzel E, Green DR. Acridine orange/ethidium bromide (AO/EB) staining to detect apoptosis. *Cold Spring Harb Protoc*. 2006. doi:10.1101/pdb.prot4493.
16. Huang T, Lin J, Cao J, Zhang P, Bai Y, Chen G, et al. An exopolysaccharide from *Trichoderma pseudokoningii* and its apoptotic activity on human leukemia K562 cells. *Carbohydr Polym*. 2012;89:701–8.
17. Kim KY, Cho HJ, Yu SN, Kim SH, Yu HS, Park YM, et al. Interplay of reactive oxygen species, intracellular Ca^{2+} and mitochondrial homeostasis in the apoptosis of prostate cancer cells by deoxyphyllotoxin. *J Cell Biochem*. 2012;114:1124–34.
18. Zhen X, Cen J, Li YM, Yan F, Guan T, Tang XZ. Cytotoxic effect and apoptotic mechanism of tanshinone A, a novel tanshinone derivative, on human erythroleukemic K562 cells. *Eur J Pharmacol*. 2011;667:129–35.
19. Liu MJ, Wang Z, Ju Y, Wong RNS, Wu QY. Diosgenin induces cell cycle arrest and apoptosis in human leukemia K562 cells with the disruption of Ca^{2+} homeostasis. *Cancer Chemother Pharmacol*. 2005;55:79–90.
20. Ausubel FM, Brent R, Kingston RE, Moore DD, Seidman J, Smith JA, et al. Short protocols in molecular biology. USA: Wiley; 1992. p. 10.8.1–10.8.23.
21. Fang L, Shen L, Fang Y, Hu Y, He Q, Yang B. MZ3 can induce G2/M-phase arrest and apoptosis in human leukemia cells. *J Cancer Res Clin Oncol*. 2008;134:1337–45.
22. Speit GN, Rothfuss A. The comet assay: a sensitive genotoxicity test for the detection of DNA damage and repair. In: Henderson DS, editors. DNA repair protocols. Totowa, New Jersey: Humana press; 2005. p. 79–90.
23. Bonner WM, Redon CE, Dickey JS, Nakamura AJ, Sedelnikova OA, Solier SP, et al. γ H2AX and cancer. *Nat Rev Cancer*. 2008;8:957–67.
24. Liu Y, Parry JA, Chin A, Duensing S, Duensing A. Soluble histone H2AX is induced by DNA replication stress and sensitizes cells to undergo apoptosis. *Mol Cancer*. 2008;7:61.
25. Brookes PS, Yoon Y, Robotham JL, Anders M, Sheu SS. Calcium, ATP, and ROS: a mitochondrial love-hate triangle. *Am J Physiol Cell Physiol*. 2004;287:C817–33.
26. Gordeeva A, Zvyagilskaya R, Labas YA. Cross-talk between reactive oxygen species and calcium in living cells. *Biochemistry (Moscow)*. 2003;68:1077–80.
27. Yan Y, Zhang WR, Cheng HP, Liu J. Cross-talk between calcium and reactive oxygen species signaling. *Acta Pharmacol Sin*. 2006;27:821–6.
28. Raj L, Ide T, Gurkar AU, Foley M, Schenone M, Li X, et al. Selective killing of cancer cells by a small molecule targeting the stress response to ROS. *Nature*. 2011;475:231–4.
29. Al-Zubairi AS, Abdul AB, Syam M. Evaluation of the genotoxicity of zerumbone in cultured human peripheral blood lymphocytes. *Toxicol in Vitro*. 2010;24:707–12.
30. Orrenius S, Zhivotovsky B, Nicotera P. Regulation of cell death: the calcium-apoptosis link. *Nat Rev Mol Cell Biol*. 2003;4:552–65.
31. Salido G. Oxidative stress, intracellular calcium signals and apoptotic processes. In: Salido GM, Rosado JA, editors. Apoptosis: involvement of oxidative stress and intracellular Ca^{2+} homeostasis. Netherlands: Springer; 2009. p. 1–16.
32. Sobhan PK, Seervi M, Deb L, Varghese S, Soman A, Joseph J, et al. Calpain and reactive oxygen species targets Bax for mitochondrial permeabilisation and caspase activation in zerumbone induced apoptosis. *PLoS ONE*. 2013;8, e59350.
33. Bauer S, Parry JA, Muhlenberg T, Brown MF, Seneviratne D, Chatterjee P, et al. Proapoptotic activity of bortezomib in gastrointestinal stromal tumor cells. *Cancer Res*. 2010;70:150–9.
34. Liu Y, Tseng M, Perdreau SA, Rossi F, Antonescu C, Besmer P, et al. Histone H2AX is a mediator of gastrointestinal stromal tumor cell apoptosis following treatment with imatinib mesylate. *Cancer Res*. 2007;67:2685–92.
35. Kang M, So E, Simons A, Spitz D, Ouchi T. DNA damage induces reactive oxygen species generation through the H2AX-Nox1/Rac1 pathway. *Cell Death Dis*. 2012;3, e249.